The Role of Shock-Flame Interactions on Flame Acceleration in an Obstacle Laden Channel

Craig Johansen and Gaby Ciccarelli,

Department of Mechanical and Materials Engineering, Queen's University, Kingston, Canada

1   Introduction

Flame acceleration in an obstacle laden channel has been investigated over the last century, most often in the context of industrial explosion safety [1]. Significant progress has been made in the last few years owing to recent advances in high-speed digital video cameras [2] and computing power [3]. The process of flame acceleration can be divided into two phases based on the importance of compressibility effects. The first phase involves flame area enhancement caused by large-scale flame distortion and small-scale turbulent fluctuations. The second phase of flame acceleration occurs at flame speeds in excess of the unburned gas speed of sound, which is approximately 350 m/s.

The results obtained from a comprehensive study carried out by Johansen and Ciccarelli [2] looking at the first phase of flame acceleration are briefly described here. The experiment studied the propagation of a flame ignited at the closed end of a square channel equipped with uniformly spaced "fence type" obstacles mounted on the top and bottom walls. The interaction of the unburned gas flow ahead of the flame with the obstacles produces a vortex downstream of each obstacle that grows in size eventually forming a recirculation zone between adjacent obstacles. The recirculation zones are isolated from the core flow by a shear layer that extends between obstacles. The shear layer and recirculation zones quickly become turbulent, but the core flow remains laminar during most of the first phase of flame acceleration. The "flame tip" propagates within the core of the channel and the remainder of the flame extends back towards the ignition end of the channel propagating transversely into the recirculation zones. As the flame tip advances forward, the total length of flame propagation in the transverse direction increases. This increase in flame area drives the increase in volumetric burning rate that is responsible for the acceleration of the flame tip.

The second phase of flame acceleration is the subject of this investigation. At flame speeds in excess of the unburned gas speed of sound, compression waves form ahead of the flame that eventually coalesce into a strong shock wave. The objective of the study is to determine the role of shock-flame interactions on flame acceleration and its effects on maximum flame tip velocity.

2   Experimental Details

The experiments were carried out in a 2.43 m long, 7.6 cm wide, square channel consisting of four equal length interchangeable modules. One of the four modules is equipped with side mounted glass windows for optical access. The optical module is placed at different positions downstream of the ignition point (module position 1) in order to capture the entire flame acceleration process. Details of

the window and instrument port locations are provided in Fig. 1. The fence type obstacles are equally spaced at the channel height. Three different obstacle heights, corresponding to flow area blockages (BR= 2h/H) of 0.33, 0.5 and 0.67, were tested. A single-pass schlieren system was used for visualization, details of which can be found in [2]. The Schlieren system uses a 35 Watt Xenon arc lamp and a Photron SA-1 high-speed digital video camera. In most of the tests the camera was operated with a 1 µs shutter. For the best quality images the camera was operated at a speed of 30,000 frames per second at a spatial pixel resolution of 704x256. The field-of-view covers roughly one-third the length of the window. All the experiments were carried out using stoichiometric methane-air at an initial pressure of 47 kPa absolute and room temperature, similar initial conditions used in the investigation reported in [2]. The mixture is prepared in a separate mixing chamber via the method of partial pressures. Ignition of the mixture is via a standard automotive ignition system.
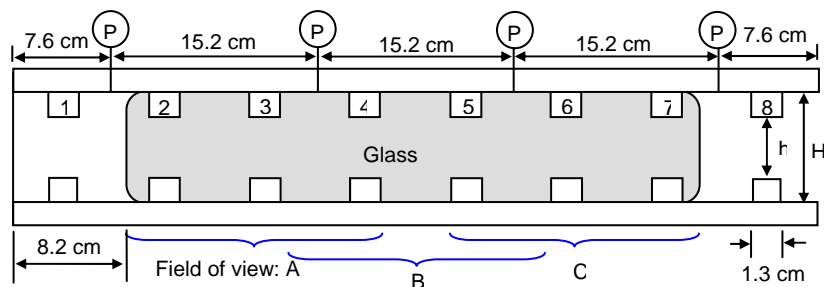

Figure 1. Schematic showing optical module and obstacle details and camera field of views

3   Results

The flame tip velocity, inferred from flame time-of-arrival measurements made at a spacing of twice the channel height, shows a monotonic increase with propagation distance [2]. The more detailed high-speed video based centerline flame velocity measurements show large oscillations for the first 0.6 m of flame acceleration up to velocities on the order of 200 m/s [2]. The flame velocity oscillations were attributed to contraction and expansion of the unburned gas flow through each obstacle pair upon which the flame tip is convected. Consequently the magnitude of the flame tip velocity oscillations were found to be greater for experiments carried out with the larger BR obstacles.

In the present study, the centerline flame velocity obtained using the high-speed camera operated at 120,000 frames per second with the optical module in position 3 and 4 is provided in Fig. 2. In order to reduce clutter, the data for the 0.67 BR obstacles is not included. However, it should be noted that the data trend is similar to that observed in tests with 0.5 BR obstacles. The data shown in Fig. 2 is a compilation from six tests for each obstacle set, i.e., one test at each field-of-view, at the two module positions. There are large oscillations in the flame tip velocity up to the end of the channel. For the 0.33 BR obstacles the magnitude of the oscillations increases dramatically in the last module position. Conversely, for the higher BR obstacles, the magnitude of the oscillations decreases near the end of the channel. The average flame tip velocity plateaus at the end of the channel at a value of about 750 m/s for the 0.5 BR and around 660 m/s for the 0.33 BR obstacles (600 m/s for the 0.67 BR obstacles). This trend in the terminal average flame velocity is consistent with flame acceleration tests made in circular tubes equipped with similar BR orifice plate obstacles [3].

Images taken from the high-speed Schlieren video obtained at 30,000 frames per second are provided in Figs. 3 and 4. For the 0.33 BR obstacles in the module 3 position, see Fig. 3a, a turbulent flame is observed to propagate through the core and no compression waves are observed ahead of the flame even though the flame tip propagates at a velocity in the range of 400 – 700 m/s. The flame velocity data in Fig. 2 shows that the flame tip accelerates as it passes through the obstacle and then quickly decelerates, similar to that observed in the early phase of flame acceleration [2]. As the flame propagates further downstream, i.e., in the module 4 location, a train of compression waves form ahead of the flame, see Fig. 3b. The compression waves reflect off the downstream top and bottom

mounted obstacles. The reflected compression waves coalesce and cross at the centerline of the channel to form a Mach stem propagating upstream. When the flame tip reaches the Mach stem just before obstacle #6 it quickly decelerates, as observed in the flame tip velocity data in Fig. 2. The flame tip then accelerates through obstacle #6 up to just before obstacle #7 where it interacts with another Mach stem. Very fine-scale perturbations appear on the flame surface as a result of the shock-flame interaction that triggers Richtmeyer-Meshkov instabilities. A flash of light is observed emanating from the interaction site which is indicative of very intense combustion. The acceleration between obstacles is due to a combination of an augmented burning rate and flow contraction.
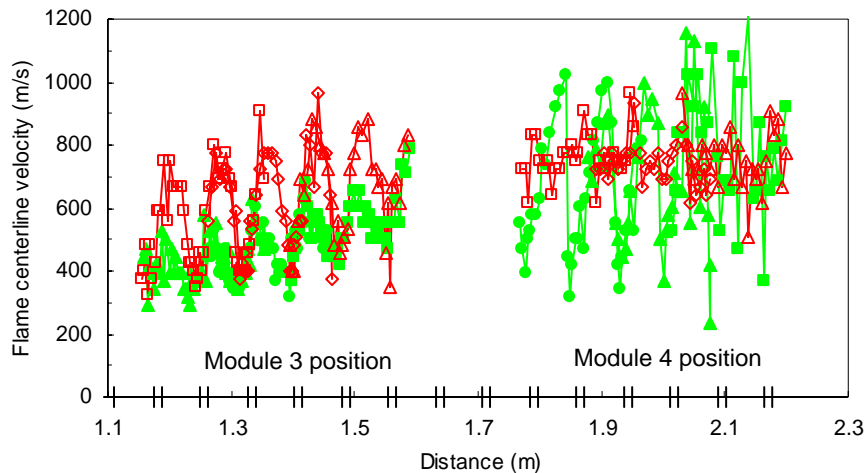

Figure 2. Flame tip velocity measured in the second half of the channel from high speed video. Obstacle positions are shown on the x-axis, data symbol designation: BR= 0.5 - open, BR= 0.33 - closed.

For the higher blockage 0.5 BR obstacles the flame initially accelerates quicker [2], which results in the formation of compression waves sooner than what is observed in experiments with the 0.33 BR obstacles. The flame-shock interactions, described above, leads to large velocity oscillations in the range of 400–900 m/s in the module 3 position. Unlike in the 0.33 BR case, the shock-flame interaction occurs before the reflected waves interact at the centerline to form a Mach stem. This allows the flame tip to follow closely behind the lead shock wave. Since a Mach stem does not form the reflected waves have less influence on the flame tip propagation, i.e., less deceleration. The flame accelerates after the shock flame interaction primarily due to flow contraction. This acceleration produces a train of compression waves that coalesce with the lead shock preventing shock decay. The shock wave first reflects off the channel top and bottom walls and then off the upstream face of the obstacles. The reflected waves propagate towards the channel centerline. Both of these reflected shock waves decelerate the flame before it reaches the channel wall and obstacle surface. This results in the consumption of the mixture near the surfaces well after the flame tip moves to the next obstacle. It should be noted that if the lead shock wave is of sufficient strength, reflection off the obstacle could lead to auto-ignition and hence an enhancement in the energy release. Transition to detonation can occur for more reactive mixtures when the shock wave becomes strong enough that shock reflection off the downstream obstacle results in detonation initiation. The obstacle reflected waves propagate as transverse waves across the flame tip, see the second image from the top in Fig. 4a. The reflection at the centerline induces a surge in the flame tip velocity up to 1000 m/s through the obstacle. This flame acceleration is short lived as the flame front propagates at roughly a constant velocity of 800 m/s across most of the span between the obstacles.

Also evident in this image is a pair of vortices and rearward facing shock waves that are typical of a Mach 2 shock wave diffracting at a 90° edge. Unlike in the first phase of the flame acceleration, the Prandtl-Meyer expansion around the obstacle permits the flame to quickly propagate towards the channel top and bottom walls. A series of compression waves form ahead of the flame, see bottom image in Fig 4a, eventually reinforcing the otherwise decaying shock wave. A very similar

shock-flame interaction is observed for the 0.67 BR obstacles, see Fig. 4b. The smaller opening results in a larger portion of the lead shock wave reflecting back towards the flame, and the portion of the shock wave that is transmitted undergoes a faster decay.

The shock-flame complex propagation at the end of the channel is quasi-steady and does not appear to involve thermal choking. The shock-flame interaction propagation mechanism appears to be self-sustaining as the flame remains closely behind the lead shock wave. The energy is released behind the shock wave within a distance equal to two or three obstacle spacing. This is very different from the first phase flame acceleration mechanism that relies principally on the extended flame area generated far behind the flame tip [2]. The shock-flame interaction mechanism is superficially similar to that of a detonation wave where the leading shock wave decays through the second half of the cell and is regenerated due to the collision of the transverse shock waves. However, they are very different because in a detonation wave the chemical reaction is shock induced.
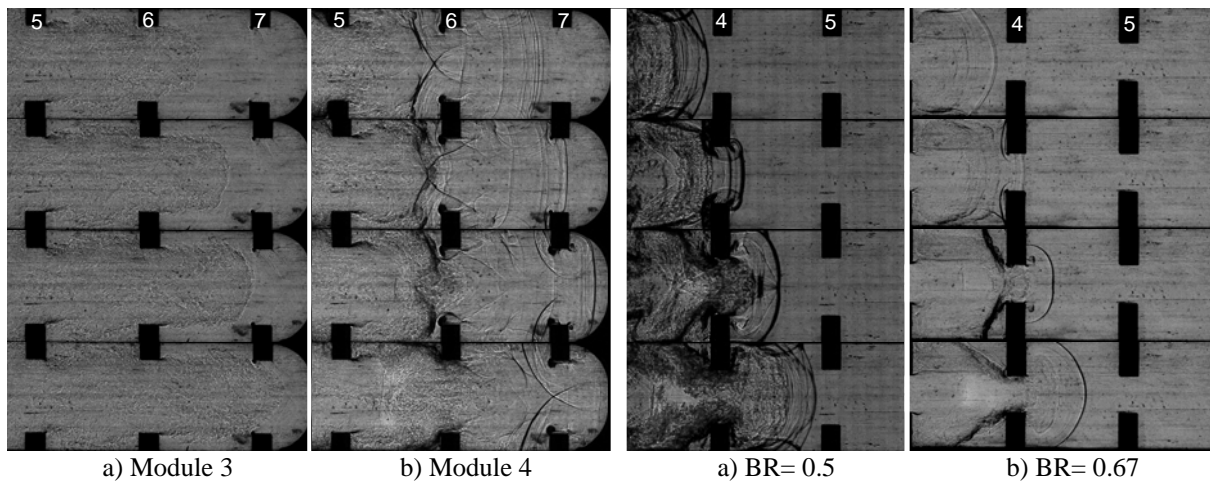

a) Module 3	b) Module 4

Figure 3. Schlieren images: 0.33 BR, field-of-view C, 33 μs inter-frame time.

a) BR= 0.5	b) BR= 0.67

Figure 4. Schlieren images: Module 4, field-of-view B, 33 μs inter-frame time.

4   Conclusions

Experiments have conclusively shown that there is a change in propagation mechanism as a flame accelerates in an obstacle laden channel. The later stages of flame acceleration are governed by shock-flame interaction, that along with flow contraction through the obstacle pair, are responsible for the observed flame tip velocity oscillations. The shock-flame interaction ultimately limits the final quasi-steady flame tip velocity, not heat and momentum losses as speculated in the literature.

References

[1] Ciccarelli G. and Dorofeev S. (2008) Flame Acceleration and Transition to Detonation in Ducts, Progress in Combustion Science, 34(4): 499-550.

[2] Johansen C. and Ciccarelli G. (2008) Visualization of the unburned gas flow field ahead of anaccelerating flame in an obstructed square channel, Combustion and Flame (DOI: 10.1016/j.combustflame.2008.07.01)

[3] Gamezo V., Takanobu O., Oran, E. (2007) Effects of obstacle spacing on flame acceleration in obstructed channels, 21st ICDERS, Poitier.

[4] Ciccarelli G., Fowler C., and Bardon M. (2005) Effects of Obstacle Size and Spacing on the Initial Stage of Flame Acceleration in a Rough Tube, Shock Waves, 14(3): 161-166.